INTERNATIONAL JOURNAL FOR NUMERICAL METHODS IN FLUIDS, VOL. 8, 1291–1318 (1988)

SIMPLE HIGH-ACCURACY RESOLUTION PROGRAM FOR CONVECTIVE MODELLING OF DISCONTINUITIES

B. P. LEONARD

Department of Mechanical Engineering, The University of Akron, Akron, Ohio, U.S.A. and ICOMP, NASA–Lewis Research Center, Cleveland, Ohio, U.S.A.

SUMMARY

For steady multi-dimensional convection, the QUICK scheme has several attractive properties. However, for highly convective simulation of step profiles, QUICK produces unphysical overshoots and a few oscillations, and this may cause serious problems in non-linear flows. Fortunately, it is possible to modify the convective flux by writing the 'normalized' convected control-volume face value as a function of the normalized adjacent upstream node value, developing criteria for monotonic resolution without sacrificing formal accuracy. This results in a non-linear functional relationship between the normalized variables, whereas standard methods are all linear in this sense. The resulting Simple High-Accuracy Resolution Program (SHARP) can be applied to steady multi-dimensional flows containing thin shear or mixing layers, shock waves and other frontal phenomena. This represents a significant advance in modelling highly convective flows of engineering and geophysical importance. SHARP is based on an explicit, conservative, control-volume flux formulation, equally applicable to one-, two-, or three-dimensional elliptic, parabolic, hyperbolic or mixed-flow regimes. Results are given for the bench-mark purely convective oblique-step test. The monotonic SHARP solutions are compared with the diffusive first-order results and the non-monotonic predictions of second- and third-order upwinding.

KEY WORDS SHARP simulation Third-order upwinding Monotonic differencing High convection Resolution of discontinuities Wiggles eliminated

INTRODUCTION

Successful modelling of strong convection is one of the most challenging problems in computational mechanics. If the truncation error terms in the numerical approximation contain second-order spatial derivatives (as in the case of first-order upwinding), simulated results are artificially diffusive and often grossly inaccurate. Central difference methods introduce propagating numerical dispersion terms (odd-order derivatives) which may corrupt large regions of the flow with unphysical oscillations. Contrary to common belief, the spatial extent of these oscillations actually increases for higher-order (central) methods. Higher-order upwind schemes have been successful in eliminating artificial diffusion, while minimizing numerical dispersion. In the case of second-order upwinding,[1] the leading truncation error is a (potentially oscillatory) third-derivative term; however, the fourth-derivative numerical dissipation is large enough to dampen short-wavelength components of the dispersion to some extent. Third-order upwinding, exemplified in the steady-state control-volume case by QUICK (Quadratic Upstream Interpolation for Convective Kinematics), has a leading fourth-derivative truncation error term which is dissipative, but higher-order dispersion terms may still cause overshoots and a few oscillations

0271–2091/88/101291–28$14.00

Received 2 November 1987
Revised 28 January 1988

when excited by (what should be) nearly discontinuous behaviour of the convected variable.[2] Currently, many general-purpose elliptic solvers (replacing those previously based on variations of essentially first-order upwinding, such as older versions of the well known TEACH code,[3] for example) are now using either second-order upwinding[4,5] or QUICK[5-20] as the basis for their convective transport solver.

QUICK, in particular, has several attractive properties: no numerical diffusion (the leading truncation error is fourth-order 'dissipation' as distinct from second-order 'diffusion'); low dispersion (the leading dispersion term is a small fifth derivative, strongly damped by the fourth-order dissipation); inherent convective stability (due to the upwinded curvature terms, even in the absence of physical diffusion); algorithmic simplicity (based on a conservative control-volume flux formulation); and computational efficiency (in terms of total 'cost' for a prescribed accuracy). QUICK also has excellent pressure prediction capabilitiy in Navier–Stokes codes; in particular, computed stagnation pressure remains constant in isentropic regions (as it should), whereas this is not the case with other convection codes.[6] Some groups using 'QUICKened' TEACH codes together with TEACH's standard tridiagonal line solver have experienced convergence problems with QUICK in strongly recirculating flow simulations.[21] However, this appears to be due to using a single sweep direction; with alternating-direction tridiagonal (or pentadiagonal) line sweeps, QUICK is extremely robust and reliable under all flow conditions.[22] Certainly, the explicit time-marching solution method described here presents no problems, even in the inviscid limit.

QUICK's single shortcoming is its tendency, under highly convective conditions, to produce overshoots and possibly some oscillations on each side of (what should be) steps in the dependent variable when convected at an angle oblique (or skew) to the grid. Even in one-dimensional flow, QUICK produces a few oscillations upstream of a sudden jump in the convected variable, under high-convection conditions. By contrast, second-order upwinding does not have this defect in one dimension; but, as seen later, this method too produces strong overshoots in two-dimensional oblique-step simulations. In some applications, small overshoots and a few oscillations may be tolerable—merely representing inaccurate resolution of the discontinuity. More likely, however, non-linear processes such as steepening in shock waves or the local behaviour of a computed diffusion or viscosity coefficient will feed back and amplify the oscillatory error, and may lead to catastrophic divergence.[13] Current practice with codes based on QUICK seems to be to revert to adding artificial diffusion in an *ad hoc* manner in order to suppress overshoots. For example, first-order upwinding might be used for k and ε equations, while QUICK is used for momentum and scalar transport[20,23]. The penalty for this 'patch-up' procedure is not immediately obvious; but, given its poor track record, one should always be suspicious of first-order upwinding.

Clearly a code retaining QUICK's desirable attributes while eliminating unphysical overshoots and oscillations would be of great practical significance. Sharp monotonic resolution of thin shear layers, species density jumps, temperature discontinuities, shock waves and other frontal phenomena is a fundamental goal of computational fluid dynamics. The following sections of this paper will show how it is possible to modify the multi-dimensional QUICK scheme to achieve this goal while retaining QUICK's third-order global accuracy and good stability characteristics; and, perhaps surprisingly, this can be done with very little additional computational cost, because the standard QUICK algorithm (or a slight variation thereof) is used throughout the overwhelming bulk of the flow domain—i.e. any (more expensive) modification is used only in thin regions requiring special treatment, thus representing only a small fraction of the overall number of grid points.

The next section describes the normalized variable diagram (NVD)—a plot of the locally normalized convected control-volume face variable with respect to the normalized adjacent

upstream node variable. In this plane, standard methods such as first- and second-order upwinding, second-order central differencing and QUICK are all represented by (different) straight lines. It will become clear that in order to satisfy both high accuracy and monotonicity, a non-linear functional relationship is necessary. The choice of this non-linear function is not unique. However, a simple scheme based on exponential upwinding has all the desired properties and is highly compatible with QUICK (both use the same grid nodes for interpolation); hence this is used as the basis for the resulting Simple High-Accuracy Resolution Program (SHARP). Details of the development of exponential upwinding are given in the second section, where it is seen that this non-linear scheme is also third-order accurate. A quantitative criterion is devised for deciding when to use the standard QUICK scheme (in 'smooth' regions) and when to invoke the more sophisticated monotonic interpolation; this quite naturally depends on the normalized curvature of the convected variable. Because exponential upwinding does not cover the entire range of the NVD, it is necessary to devise *ad hoc* extensions to match with QUICK at the extreme ranges; this is achieved *via* simple piecewise linear constructions, resulting in what has become known as the Exponential Upwinding or Linear Extrapolation Refinement (EULER). This section closes with a sketch of the EULER–QUICK algorithm in one dimension, for clarity. The following section outlines the two-dimensional algorithm in detail and shows how it can easily be extended to three-dimensional steady flow. Finally, results are given for the well known bench-mark two-dimensional pure-convection oblique-step test—probably the most severe test for any convection scheme. This is used for a direct comparison between classical first-order upwinding, second-order upwinding, QUICK and SHARP. As expected, first-order upwinding is extremely artificially diffusive. Rather surprisingly, second-order upwinding exhibits quite strong overshoots at some convection angles. QUICK gives steeper resolution of the jump region, but generates angle-dependent overshoots and some oscillations. By dramatic contrast, SHARP retains the steep resolution of QUICK but remains absolutely monotonic. Its overall characteristics seem virtually insensitive to flow-to-grid angle.

NORMALIZED VARIABLE DIAGRAM

Definition of normalized variables

Consider the variation of a convected scalar $\phi(x, y, z)$ along a direction normal to a control-volume (CV) face, as shown in Figure 1(a). For the CV face convecting velocity direction shown, QUICK involves the two adjacent node values (ϕ_D and ϕ_C) together with that at the next upstream node (ϕ_U) in modelling the convected CV face value ϕ_f. Note that the labelling of node values—downstream (D), central (C) and upstream (U)—depends on the normal velocity direction, as of course does the choice of node for ϕ_U. Figure 1(b) shows the same information in terms of the locally normalized variable

$$\tilde{\phi}=\frac{\phi-\phi_U}{\phi_D-\phi_U}. \tag{1}$$

Note particularly that, in terms of normalized variables, $\tilde{\phi}_D=1$ and $\tilde{\phi}_U=0$.

For example, for QUICK, on a uniform grid, the convected CV face variable is[2]

$$\phi_f=\tfrac{1}{2}(\phi_D+\phi_C)-\tfrac{1}{8}(\phi_D-2\phi_C+\phi_U), \tag{2}$$

so, in terms of normalized variables,

$$\tilde{\phi}_f=\tfrac{1}{2}(1+\tilde{\phi}_C)-\tfrac{1}{8}(1-2\tilde{\phi}_C+0) \tag{3}$$

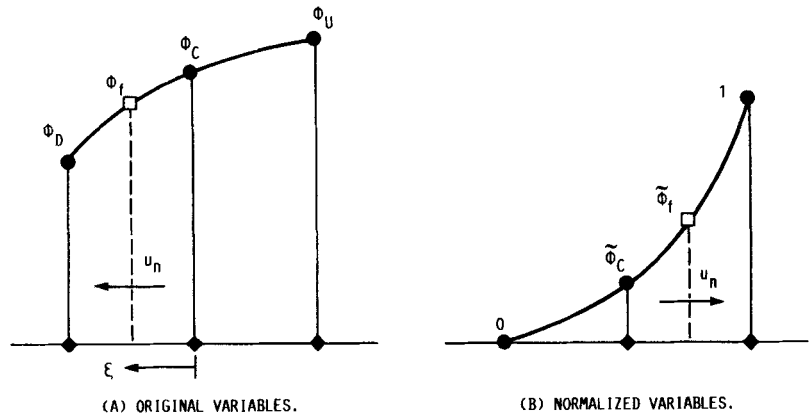

Figure 1. Node variables in the vicinity of a CV face (at dashed line): (a) original variables; (b) normalized variables

or, more conveniently,

QUICK

$$\tilde{\phi}_f = 0{\cdot}75 + 0{\cdot}75(\tilde{\phi}_C - 0{\cdot}5). \tag{4}$$

It should be clear that if ϕ_f is a function of ϕ_D, ϕ_C and ϕ_U, then the normalized variable $\tilde{\phi}_f$ is only a function of $\tilde{\phi}_C$ (since $\tilde{\phi}_D = 1$ and $\tilde{\phi}_U = 0$). This is the basis of the normalized variable diagram (NVD), which is a plot of the functional relationship between the normalized convected face value $\tilde{\phi}_f$ and the normalized adjacent upstream node value $\tilde{\phi}_C$.

Linear schemes

Equation (4) shows that, for QUICK, the normalized variable diagram is a straight line passing through (0·5, 0·75) with a slope of 0·75. Other well known schemes also have linear characteristics. For example, first-order upwinding requires, using the present notation (which takes account of flow direction), zeroth-order upwind 'interpolation'

$$\phi_f = \phi_C \tag{5}$$

or, in terms of normalized variables, simply

first-order upwinding

$$\tilde{\phi}_f = \tilde{\phi}_C. \tag{6}$$

Similarly, second-order central differencing, being independent of SGN(u_n), is simply the linear interpolation

$$\phi_f = \tfrac{1}{2}(\phi_D + \phi_C), \tag{7}$$

which becomes, in terms of normalized variables,

second-order central

$$\tilde{\phi}_f = 0{\cdot}75 + 0{\cdot}5(\tilde{\phi}_C - 0{\cdot}5); \tag{8}$$

and second-order upwinding, given by linear upwind-biased extrapolation

$$\phi_f = \tfrac{3}{2}\phi_C - \tfrac{1}{2}\phi_U, \tag{9}$$

can be written

second-order upwinding

$$\tilde{\phi}_f = \tfrac{3}{2}\tilde{\phi}_C. \tag{10}$$

The linear NVD characteristics, equations (4), (6), (8) and (10), are shown in Figure 2(a). The corresponding normalized interpolations are shown in Figure 2(b) for a specific value of $\tilde{\phi}_C (< 0{\cdot}5)$. Note that three of the characteristics pass through the point (0·5, 0·75), labelled Q. First-order upwinding passes through the origin O and the point P at (1, 1), but it passes well below Q.

Characteristics passing through Q can be written

$$\tilde{\phi}_f = 0{\cdot}75 + S(\tilde{\phi}_C - 0{\cdot}5), \tag{11}$$

where S represents the slope of the line. Using the original (un-normalized) variables, these can be written in terms of the (upstream-weighted) curvature

$$\phi_f = 0{\cdot}5(\phi_D + \phi_C) - \mathrm{CF}(\phi_D - 2\phi_C + \phi_U), \tag{12}$$

where CF is the curvature factor.

Clearly, $S = 2\mathrm{CF} + 0{\cdot}5$, and in specific cases

QUICK

$$\mathrm{CF} = \tfrac{1}{8}, \qquad S = \tfrac{3}{4}, \tag{13}$$

second-order central

$$\mathrm{CF} = 0 \qquad S = \tfrac{1}{2}, \tag{14}$$

second-order upwind

$$\mathrm{CF} = \tfrac{1}{2}, \qquad S = \tfrac{3}{2}. \tag{15}$$

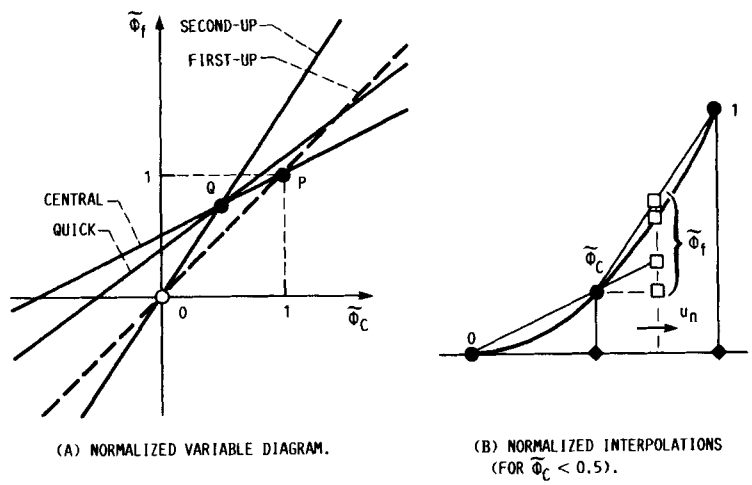

(A) NORMALIZED VARIABLE DIAGRAM.

(B) NORMALIZED INTERPOLATIONS (FOR $\tilde{\Phi}_C < 0.5$).

Figure 2. First-order upwinding, second-order upwinding, second-order central differencing and third-order upwinding (QUICK): (a) normalized variable diagram; (b) normalized interpolations (for $\tilde{\phi}_C < 0{\cdot}5$)

In terms of normalized variables, equation (12) becomes

$$\tilde{\phi}_f = 0{\cdot}5(1+\tilde{\phi}_C) - CF(1-2\tilde{\phi}_C). \tag{16}$$

Note that, in general, any (non-linear) functional relationship between $\tilde{\phi}_f$ and $\tilde{\phi}_C$ passing through Q can be written in the form of equation (16) provided CF is taken to be a function of $\tilde{\phi}_C$ rather than a constant. Also, by making a Taylor series expansion about the CV face locations, it is not difficult to show that for any (in general, non-linear) characteristic

(i) passing through Q is necessary and sufficient for second-order accuracy
(ii) passing through Q with a slope of $\frac{3}{4}$ is necessary and sufficient for third-order accuracy.

This means that any scheme based on a characteristic which can be written in the form of equation (16), with $CF = CF(\tilde{\phi}_C)$, is at least second-order accurate; and if

$$CF(0{\cdot}5) = 0{\cdot}125 \leftrightarrow S(0{\cdot}5) = 0{\cdot}75, \tag{17}$$

the scheme is third-order accurate. This, of course, correlates with equations (13)–(15), which show that the simple second-order schemes pass through Q with a slope other than $\frac{3}{4}$, whereas the third-order QUICK scheme indeed has $S = \frac{3}{4}$. Note that first-order upwinding cannot be written in the form of equation (16), since it does not pass through Q. The non-linear NVD characteristic to be developed in the next section will pass through Q with a slope of $\frac{3}{4}$, thus maintaining formal third-order accuracy.

In the Appendix it is shown that linear NVD characteristics which pass through the second quadrant may produce unphysical oscillations in steady one-dimensional convection. This is a well known failing of central differencing and may also occur to some extent with QUICK under high-convection conditions.[2] From Figure 2(a) one sees immediately that these two characteristics indeed pass through the second quadrant. Experience has shown that such schemes are also oscillatory in two-dimensional steady-flow simulations. Characteristics which pass through the fourth quadrant (i.e. below O) are artificially diffusive. Thus, in order to avoid oscillations without being artificially diffusive, one necessary condition for the non-linear characteristic to satisfy is that it must pass through the origin O. Numerical experimentation has also shown that NVD characteristics which pass above P are oscillatory in two dimensions (although not necessarily so in one dimension—second-order upwinding being the classic example). Similarly, passing below P gives artificially diffusive results. So another necessary condition for the non-linear characteristic is that it must pass through P. Behaviour of the non-linear scheme to be developed can be summarized for the monotonic regime ($0 \leq \tilde{\phi}_C \leq 1$):

The non-linear NVD characteristic should pass through O, P and Q, with a slope of $\frac{3}{4}$ at Q.

For $\tilde{\phi}_C$-values less than 0 or greater than 1, the characteristic should be extended in a continuous manner, ultimately approaching the QUICK line for extreme values. The next section outlines the development of a scheme which satisfies the above criteria.

EXPONENTIAL UPWINDING OR LINEAR EXTRAPOLATION REFINEMENT

Exponential upwinding

Quadratic upstream interpolation is based on assumed local behaviour of the form

$$\phi = a + b\xi + c\xi^2, \tag{18}$$

where ξ is a local spatial co-ordinate normal to the CV face, positive in the direction of the convecting velocity, as seen in Figure 1(a). Evaluating a, b and c in terms of the local node values results in

QUICK

$$\phi(\xi)=\phi_C+\left(\frac{\phi_D-\phi_U}{2\Delta x}\right)\xi+\left(\frac{\phi_D-2\phi_C+\phi_U}{2\Delta x^2}\right)\xi^2; \tag{19}$$

and, of course, setting $\xi=\Delta x/2$ results in equation (2) for ϕ_f.

Now consider an entirely different type of interpolation through the same three node values, based on an assumed (upstream-weighted) exponential of the form

$$\phi(\xi)=A+B\exp(C\xi). \tag{20}$$

Evaluating the three parameters in terms of node values leads to

$$\phi(0)=\phi_C=A+B, \tag{21}$$

$$\phi(-\Delta x)=\phi_U=A+B\,e^{-C\Delta x}, \tag{22}$$

$$\phi(\Delta x)=\phi_D=A+B\,e^{C\Delta x}, \tag{23}$$

from which it is easily found that

$$A=\frac{\phi_D\phi_U-\phi_C^2}{\phi_D-2\phi_C+\phi_U} \tag{24}$$

and

$$\phi(\Delta x/2)=\phi_f=A\pm\sqrt{(\phi_D-A)(\phi_U-A)} \tag{25}$$

or, in terms of normalized variables,

$$\tilde{\phi}_f=\frac{\sqrt{\tilde{\phi}_C(1-\tilde{\phi}_C)^3}-\tilde{\phi}_C^2}{1-2\tilde{\phi}_C}, \tag{26}$$

with no ambiguity of sign on the square root. This represents the desired exponential upwinding (EU) characteristic for the normalized variable diagram. Note that it is defined only in the monotonic regime ($0\le\tilde{\phi}_C\le 1$). There is an indeterminacy at $\tilde{\phi}_C=0{\cdot}5$; but it is easy to show, using L'Hôpital's rule, that

$$\tilde{\phi}_f(0{\cdot}5)=0{\cdot}75. \tag{27}$$

Similarly, straightforward differentiation results in

$$\left(\frac{\partial\tilde{\phi}_f}{\partial\tilde{\phi}_C}\right)_{EU}=S(EU)=0{\cdot}75 \quad \text{at } \tilde{\phi}_C=0{\cdot}5, \tag{28}$$

showing that exponential upwinding is tangent to the QUICK line at $\tilde{\phi}_C=0{\cdot}5$. This means, of course, that exponential upwinding is third-order accurate. The exponential upwinding characteristic is shown in Figure 3(a) in relation to QUICK (dashed), while Figure 3(b) shows the corresponding normalized EU and QUICK interpolations for a small positive value of $\tilde{\phi}_C$ with the corresponding $\tilde{\phi}_f$ values shown in Figure 3(a).

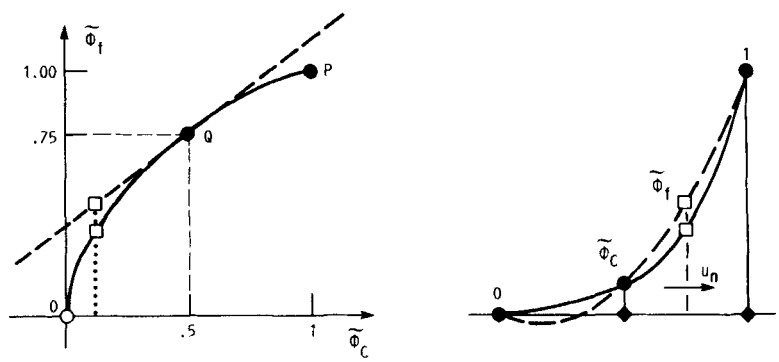

Figure 3. Exponential upwinding (solid curves) shown in relation to QUICK (dashed): (a) normalized variable diagram; (b) normalized interpolations

Modification criterion

Note that the EU curve lies quite close to QUICK over a fairly wide range near $\tilde{\phi}_C \sim 0{\cdot}5$. This suggests a very simple modification strategy for deciding whether to use the basic QUICK scheme or the more sophisticated interpolation:

$$\text{if} \quad |0{\cdot}5 - \tilde{\phi}_C| \leq \text{const}, \quad \text{use QUICK}, \tag{29}$$

where from Figure 3(a) a value of const $= 0{\cdot}15$ might be considered reasonable. Multiplying by 2, this becomes

$$\text{if} \quad |1 - 2\tilde{\phi}_C| \leq 0{\cdot}3, \quad \text{use QUICK}, \tag{30}$$

or more directly, when written in terms of un-normalized variables,

$$\text{if} \quad |\phi_U - 2\phi_C + \phi_D| \leq 0{\cdot}3 |\phi_D - \phi_U|, \quad \text{use QUICK}. \tag{31}$$

Since the left-hand side of this equation is proportional to the curvature (normal to the CV face) of the convected variable, the modification criterion is a quantitative statement of the desire to use QUICK in 'smooth' (i.e. small-curvature) regions of the flow domain. This will be the case in the bulk of the flow, since high curvature (rapid change in gradient) occurs only in thin regions involving a small number of grid points. Thus, although exponential upwinding is more expensive than QUICK, it is only used in a small fraction of the computational domain (if at all), so that the overall strategy is extremely cost-effective.

Non-monotonic regime

Since exponential upwinding is only available in the monotonic regime, the question remains as to the best procedure to adopt for $\tilde{\phi}_C \geq 1$ and $\tilde{\phi}_C \leq 0$. For $\tilde{\phi}_C$ above 1, a simple and apparently robust strategy is to use the continuous extension

$$\tilde{\phi}_f = \tilde{\phi}_C \quad \text{for } 1 \leq \tilde{\phi}_C \leq 1{\cdot}5, \tag{32}$$

returning (again without loss of continuity) to QUICK at $\tilde{\phi}_C \geq 1{\cdot}5$. Note that, although this portion of the overall non-linear NVD characteristic happens to coincide with that of first-order upwinding, it does not degrade the order of the overall algorithm—which is determined solely by equations (27) and (28). The whole concept of 'order' based on Taylor series only has meaning for

smooth behaviour near $\tilde{\phi}_C \to 0{\cdot}5$ (i.e. vanishing curvature). Statements such as those often made in relation to TVD schemes[24] (that such schemes are only first-order accurate near extrema: $\tilde{\phi}_C \leq 0$ or ≥ 1 in the present notation) are totally meaningless and can be quite misleading. What is actually meant is that, in the present notation, $\tilde{\phi}_f = \tilde{\phi}_C$ for $\tilde{\phi}_C \leq 0$ and $\tilde{\phi}_C \geq 1$, which happens to coincide with the first-order upwinding characteristic in the non-monotonic regime, but not (necessarily) near $\tilde{\phi}_C \to 0{\cdot}5$.

The negative-$\tilde{\phi}_C$ regime requires somewhat more care in designing an extension from exponential upwinding, which ends at (0, 0). A characteristic which rejoins QUICK at some finite negative $\tilde{\phi}_C$-value seems desirable; this could be done with a straight-line characteristic through (0, 0) with a slope less than $\frac{3}{4}$. However, it is important to avoid a certain critical point on the QUICK characteristic (at $\tilde{\phi}_C = -\sqrt{(3/2)}$), since, as shown in the Appendix, traversing this point on the QUICK line could lead to unphysical oscillations under certain circumstances. It is thus better to rejoin the QUICK line below the critical point. This is adequately accomplished by the *ad hoc* straight-line characteristic

$$\tilde{\phi}_f = \tfrac{3}{8}\tilde{\phi}_C \quad \text{for } -1 \leq \tilde{\phi}_C \leq 0 \tag{33}$$

continuing along the QUICK line for $\tilde{\phi}_C \leq -1$. The complete composite NVD characteristic is shown in Figure 4, representing an Exponential Upwinding or Linear Extrapolation Refinement of QUICK.

The EULER–QUICK algorithm

The one-dimensional algorithm is summarized here for reference for each CV face:

(i) Designate upstream and downstream nodes on the basis of SGN(u_n).
(ii) If $|\phi_D - \phi_U| < 10^{-5}$ (say), use QUICK, otherwise
(iii) Check if inequality (31) is satisfied (this will account for the bulk of the flow field).

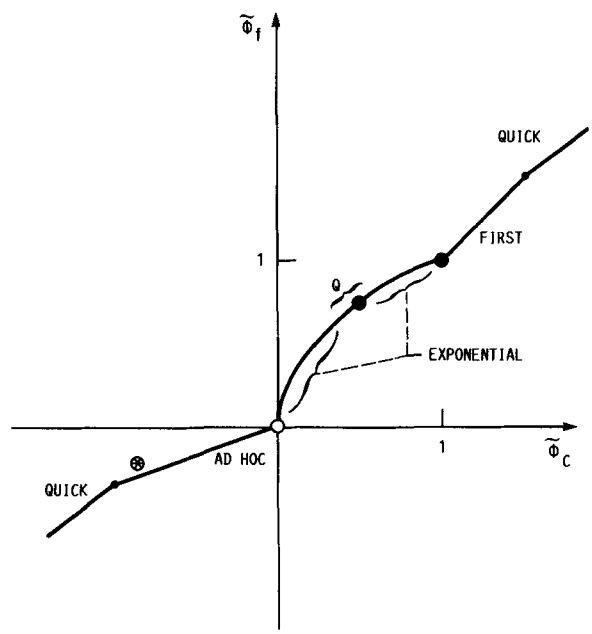

Figure 4. Composite NVD characteristic for the EULER–QUICK scheme

(iv) If not, compute $\tilde{\phi}_C=(\phi_C-\phi_U)/(\phi_D-\phi_U)$ and find $\tilde{\phi}_f$ by
(v) QUICK, equation (4), if $\tilde{\phi}_C\le -1$ or $\tilde{\phi}_C\ge 1{\cdot}5$, or if $0{\cdot}35\le\tilde{\phi}_C\le 0{\cdot}65$,
(vi) $\tilde{\phi}_f=0{\cdot}375\tilde{\phi}_C$ if $-1<\tilde{\phi}_C\le 0$,
(vii) exponential upwinding, equation (26), for $0<\tilde{\phi}_C<0{\cdot}35$ and for $0{\cdot}65<\tilde{\phi}_C\le 1$, or
(viii) $\tilde{\phi}_f=\tilde{\phi}_C$ for $1<\tilde{\phi}_C\le 1{\cdot}5$.
(ix) Then reconstruct the (un-normalized) face value $\phi_f=\phi_U+(\phi_D-\phi_U)\tilde{\phi}_f$.

In this way the convective flux at the left face can be computed as

$$\mathrm{CFLUXL}(i)=\mathrm{CXL}(i)\cdot\phi_f, \tag{34}$$

where $\mathrm{CXL}(i)=u_n(i)\Delta t/\Delta x$ is the local normal velocity component Courant number at the left face for CV(i). Because of the conservative CV formulation, the right-face flux at CV(i) is just the left-face flux at CV($i+1$), regardless of velocity direction. The explicit update algorithm for pure convection then becomes, quite simply,

$$\phi_i^{n+1}=\phi_i^n+\mathrm{CFLUXL}(i)-\mathrm{CFLUXL}(i+1). \tag{35}$$

In the steady state, of course, $\phi_i^{n+1}=\phi_i^n$, so that the FLUX terms must balance. Diffusive flux terms are treated in an analogous fashion (using $\mathrm{DXL}=\Gamma_e\Delta t/\Delta x^2$, Γ being a diffusion coefficient or viscosity):

$$\mathrm{DFLUXL}(i)=\mathrm{DXL}(i)\cdot(\phi_i-\phi_{i-1}), \tag{36}$$

involving the simple linear difference across the left face, which is consistent with the third-order treatment of the convective fluxes.[2] Control-volume-averaged source terms can be added if appropriate.

MULTI-DIMENSIONAL ALGORITHM: SHARP

Two-dimensional QUICK scheme

Figure 5 shows a two-dimensional control volume, with attention focused on convection across the left face. In the situation shown, u_l is positive to the right, so for a control volume centred at node (i, j) the following designation of upstream and downstream variables results, in the direction normal to the face:

$$\phi_D=\phi(i,j),\qquad \phi_C=\phi(i-1,j),\qquad \phi_U=\phi(i-2,j)\quad \text{for } u_l>0; \tag{37}$$

and the upstream-weighted transverse nodes are

$$\phi_T=\phi(i-1,j+1),\qquad \phi_B=\phi(i-1,j-1)\quad \text{for } u_l>0. \tag{38}$$

It should be clear which nodes would be involved for $u_l<0$.

For the basic two-dimensional QUICK scheme,[25] the convected value averaged at the left face is (for $u_l>0$)

$$\phi_l=\tfrac{1}{2}(\phi_D+\phi_C)-\tfrac{1}{8}(\phi_D-2\phi_C+\phi_U)+\tfrac{1}{24}(\phi_T-2\phi_C+\phi_B), \tag{39}$$

which includes the linear interpolation term, the upstream normal curvature term and a small term representing the effect of (upstream-biased) transverse curvature in computing the face average. Note that the first two terms are identical with the one-dimensional formula, equation (2). Thus one possible strategy for the two-dimensional SHARP is to follow the one-dimensional algorithm, steps (i)–(ix) above, for each left face, and then simply add the appropriate transverse

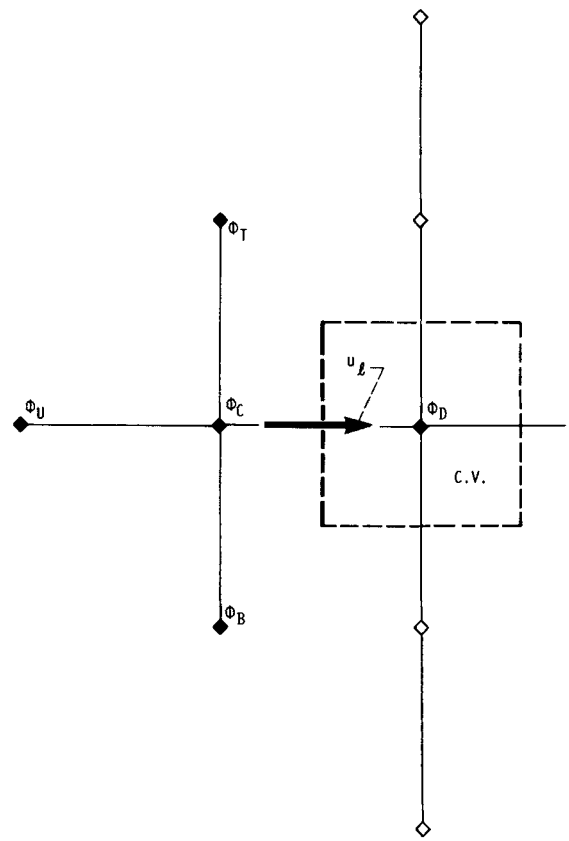

Figure 5. Two-dimensional control volume showing nodes involved in estimating the average left-face value for $u_l > 0$

curvature term (depending in the sign of u_l); a similar procedure is used for the bottom faces. One needs to store left-face (convective plus diffusive) fluxes

$$\text{FLUXL}(i,j) = \text{CXL}(i,j) \cdot \phi_l - \text{DXL}(i,j) \cdot [\phi(i,j) - \phi(i-1,j)] \tag{40}$$

and bottom-face fluxes

$$\text{FLUXB}(i,j) = \text{CYB}(i,j) \cdot \phi_b - \text{DYB}(i,j) \cdot [\phi(i,j) - \phi(i,j-1)]. \tag{41}$$

The explicit update algorithm is then extremely simple, using an overwriting assignment statement

$$\begin{aligned} \text{set:} \quad \phi(i,j) = {} & \phi(i,j) + \Delta t\, S^*(i,j) \\ & + \text{FLUXL}(i,j) - \text{FLUXL}(i+1,j) \\ & + \text{FLUXB}(i,j) - \text{FLUXB}(i,j+1), \end{aligned} \tag{42}$$

where S^* is the CV-averaged source term. Note that, in terms of storage requirements, it is necessary to store two flux arrays for each transport variable.

Curvature-based algorithm

An alternative strategy, that can be used for one-, two-, or three-dimensional simulations, is to write for the average left-face convected value (suppressing j and k indices, for convenience)

$$\phi_l=\tfrac{1}{2}(\phi_i+\phi_{i-1})-\mathrm{CF}\cdot\mathrm{CURVN}+\tfrac{1}{24}(\mathrm{CURVTY}+\mathrm{CURVTZ}), \tag{43}$$

where CURVTY and CURVTZ are the respective upstream-weighted transverse curvature terms in the other co-ordinate directions, and the upstream-biased normal curvature can be written

$$\mathrm{CURVN}=\tfrac{1}{2}(\phi_{i+1}-\phi_i-\phi_{i-1}+\phi_{i-2})-\tfrac{1}{2}\mathrm{SGN}(u_l)\cdot(\phi_{i+1}-3\phi_i+3\phi_{i-1}-\phi_{i-2}), \tag{44}$$

which takes account of the velocity direction automatically. For the standard QUICK algorithm, of course, the normal curvature factor, CF in equation (43), is a constant ($=\frac{1}{8}$). The explicit SHARP algorithm can be implemented simply by writing, from equation (16),

$$\mathrm{CF}=\mathrm{CF}(\tilde{\phi}_\mathrm{C})=\frac{\tilde{\phi}_\mathrm{f}(\tilde{\phi}_\mathrm{C})-0{\cdot}5(1+\tilde{\phi}_\mathrm{C})}{2\tilde{\phi}_\mathrm{C}-1}, \tag{45}$$

which is shown in Figure 6, along with the non-monotonic extensions, corresponding to the complete NVD characteristic of Figure 4.

Again the algorithm begins by computing $|\phi_\mathrm{D}-\phi_\mathrm{U}|$ and going immediately to QUICK if this is less than a specified small number. If not, one computes $\tilde{\phi}_\mathrm{C}$ in the usual way and then goes to algebraic expressions representing the behaviour shown in Figure 6 for $\mathrm{CF}(\tilde{\phi}_\mathrm{C})$ as follows:

for $\tilde{\phi}_\mathrm{C}\le -1$ or $\tilde{\phi}_\mathrm{C}\ge 1{\cdot}5$, $\quad \mathrm{CF}=0{\cdot}125;$ (46)

for $-1<\tilde{\phi}_\mathrm{C}\le 0$, $\quad \mathrm{CF}=(0{\cdot}5+0{\cdot}125\tilde{\phi}_\mathrm{C})/(1-2\tilde{\phi}_\mathrm{C});$ (47)

for $1\le\tilde{\phi}_\mathrm{C}<1{\cdot}5$, $\quad \mathrm{CF}=\tfrac{1}{2}(\tilde{\phi}_\mathrm{C}-1)/(2\tilde{\phi}_\mathrm{C}-1);$ (48)

for $0{\cdot}3\le\tilde{\phi}_\mathrm{C}\le 0{\cdot}7$, use the quadratic approximation

$$\mathrm{CF}=0{\cdot}125-0{\cdot}2609(\tilde{\phi}_\mathrm{C}-1{\cdot}5)+0{\cdot}13613(\tilde{\phi}_\mathrm{C}-0{\cdot}5)^2; \tag{49}$$

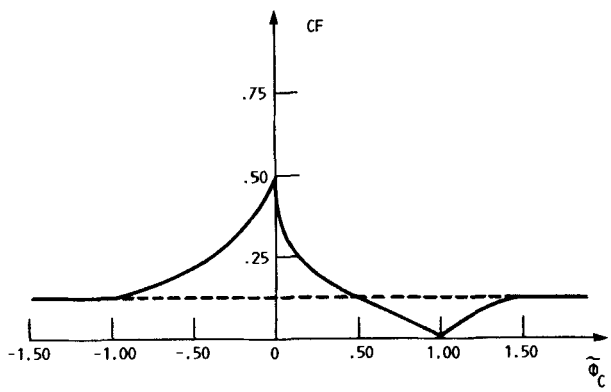

Figure 6. Normal curvature factor CF as a function of the normalized upstream node value $\tilde{\phi}_\mathrm{C}$ for the EULER–QUICK scheme (corresponding to Figure 4)

and finally, for $0<\tilde{\phi}_C<0{\cdot}3$ and $0{\cdot}7<\tilde{\phi}_C<1$, use the exact exponential upwinding formula, combining equations (26) and (45),

$$\mathrm{CF}=\frac{\tilde{\phi}_C^2-(1+\tilde{\phi}_C)(\tilde{\phi}_C-0{\cdot}5)-\sqrt{\tilde{\phi}_C(1-\tilde{\phi}_C)^3}}{(1-2\tilde{\phi}_C)^2}. \tag{50}$$

It should be clear that most of the grid points will be in the smooth region ($\tilde{\phi}_C\to 0{\cdot}5$) and thus will involve equation (49). This empirical formula is graphically indistinguishable from the exact EU curve in this region. A less expensive strategy uses the following approximate formulae, in addition to equation (46):

$$\text{for } -1<\tilde{\phi}_C\le 0, \qquad \mathrm{CF}=\tfrac{1}{2}+\tfrac{3}{8}\tilde{\phi}_C; \tag{51}$$

$$\text{for } 0<\tilde{\phi}_C\le \tfrac{1}{4}; \qquad \mathrm{CF}=\tfrac{1}{2}-\tfrac{5}{8}\sqrt{\tilde{\phi}_C}; \tag{52}$$

$$\text{for } \tfrac{1}{4}<\tilde{\phi}_C\le 1; \qquad \mathrm{CF}=\tfrac{1}{4}(1-\tilde{\phi}_C); \tag{53}$$

$$\text{for } 1<\tilde{\phi}_C\le \tfrac{3}{2}; \qquad \mathrm{CF}=\tfrac{1}{4}(\tilde{\phi}_C-1). \tag{54}$$

In this case most grid points will involve the simple linear formula given in equation (53). Note that $\mathrm{CF}=\frac{1}{8}$ when $\tilde{\phi}_C=\frac{1}{2}$, thus maintaining third-order accuracy even in this simple approximate scheme. The main difference between equations (47)–(50) and equations (51)–(54) is that in the latter case the monotonic extensions are approximated by straight lines for $\mathrm{CF}(\tilde{\phi}_C)$ rather than by segments of hyperbolae; since this is an *ad hoc* procedure in either case, the exact shape of these extensions is immaterial, provided they revert to the QUICK value ($\mathrm{CF}=\frac{1}{8}$) in a reasonable manner (and avoid the critical point).

Extension to three dimensions

The three-dimensional algorithm parallels the two-dimensional version, simply adding the upstream-biased transverse curvature for the third direction and then setting up (convective plus diffusive) fluxes for 'left' (L), 'bottom' (B) and 'far' (F) faces of each CV cell. The explicit update then becomes

$$\begin{aligned}\text{set: } \phi(i,j,k)=\phi(i,j,k)&+\Delta t\, S^*(i,j,k)\\&+\mathrm{FLUXL}(i,j,k)-\mathrm{FLUXL}(i+1,j,k)\\&+\mathrm{FLUXB}(i,j,k)-\mathrm{FLUXB}(i,j+1,k)\\&+\mathrm{FLUXF}(i,j,k)-\mathrm{FLUXF}(i,j,k+1),\end{aligned} \tag{55}$$

where, as usual, flux consistency is guaranteed by the control-volume formulation; e.g. the 'near' face flux FLUXN (i,j,k) has been replaced by FLUXF$(i,j,k+1)$. In the three-dimensional case, of course, it is necessary to store three flux arrays for each transport variable.

Numerical boundary conditions

As a general principle, QUICK boundary condition treatment is used;[25] i.e. quadratic extrapolation normal to the boundary to set up external pseudo-node values, using the given physical conditions together with enough interior node values to perform the extrapolation. This works well for all transport variables unless there is a discontinuity oblique to the grid very close to the boundary. In such a case the classic solution of local mesh refinement can be used. Alternatively, other high-resolution forms of local behaviour can be developed on a case-by-case basis. For example, boundary layer flow with a no-slip condition and strong pressure gradient can

be modelled on a relatively coarse grid in a manner compatible with QUICK (and SHARP) by assuming a local behaviour normal to the wall such as

$$u = C_1 y^{1/n} + C_2 y, \tag{56}$$

i.e. a power-law-plus-linear profile with an assumed value of n. This is really a three-point interpolation since the condition $u(0)=0$ has already been assumed; it would replace the usual (three-point) quadratic variation (used in QUICK)

$$u = c_1 y + c_2 y^2, \tag{57}$$

again assuming $u(0)=0$. In each case the coefficients are computed using two internal node values normal to the wall. Equation (56) allows much more rapid variation in the CV cell adjacent to the wall; it can be used in the same spirit as logarithmic wall functions.[3] Naturally, details regarding convective and diffusive fluxes need to be worked out in individual cases, but this is a straightforward matter.

At inflow boundaries it is sometimes convenient to set up two external pseudo-nodes so that the usual (internal) QUICK or SHARP algorithm can be used directly. Figure 7 shows a situation in which ϕ_{BC} is given at an inflow boundary. Local quadratic behaviour in terms of the distance from the first interior node implies

$$\phi(\xi) = \phi_3 + \left(\frac{\phi_4 - \phi_2}{2\Delta x}\right)\xi + \left(\frac{\phi_4 - 2\phi_3 + \phi_2}{2\Delta x^2}\right)\xi^2, \tag{58}$$

thus

$$\phi_{BC} = \phi(-\Delta x/2) = \phi_3 - \tfrac{1}{4}(\phi_4 - \phi_2) + \tfrac{1}{8}(\phi_4 - 2\phi_3 + \phi_2). \tag{59}$$

Solving for ϕ_2 gives

$$\phi_2 = \tfrac{8}{3}\phi_{BC} - 2\phi_3 + \tfrac{1}{3}\phi_4 \tag{60}$$

and, since for a quadratic function the third difference is zero, ϕ_1 is given by

$$\phi_1 = 3\phi_2 - 3\phi_3 + \phi_4. \tag{61}$$

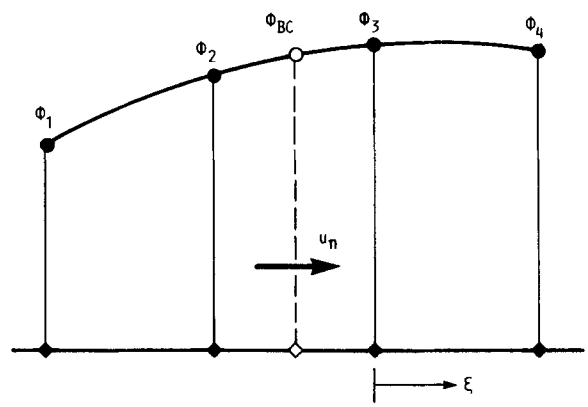

Figure 7. Numerical boundary conditions at an inflow boundary

For outflow conditions one may assume zero local curvature in the flow direction unless other physical conditions are specified. This is clearly not as restrictive as zero local gradient and may allow the use of smaller computational domains for a given accuracy.

Time-step restrictions

If one makes a classical von Neumann analysis of the (one-dimensional) QUICK scheme, assuming unsteady convection and diffusion in an infinite domain, the resulting time-step restrictions are rather stringent.[26] In fact the convection-controlled restriction is formally the same as the simple forward time/central space requirement[27] on the Courant number ($c = u\Delta t/\Delta x$),

$$c \leq 2/P_\Delta, \tag{62}$$

where $P_\Delta = u\Delta x/\Gamma$ is the grid Peclet number (or Reynolds number). This would imply, of course, that purely convective flow ($P_\Delta \to \infty$) could not be simulated by the explicit QUICK scheme. Fortunately, the formal von Neumann analysis does not apply to steady-state algorithms on a finite grid. In particular, since the instability indicated by violating equation (62) is at the long-wavelength end of the Fourier spectrum, the imposition of a long-wavelength cut-off (corresponding to a finite grid) results in a much less restrictive condition.[27] This can be written in an accurate simplified form as[25]

$$c \leq \frac{2}{P_\Delta} + \frac{\pi^2}{2N^2}, \tag{63}$$

where $N\Delta x = \lambda^*$, the cut-off wavelength, from which it can be seen that even in the 'inviscid' limit ($P_\Delta \to \infty$) there is always a non-zero time step available for explicit solution of the QUICK algorithm on a finite grid. Even this can be violated when using time-marching toward a steady-state solution, because any unstable modes tend to be suppressed by the steady-state boundary conditions. Finally, the non-linearity of the SHARP scheme allows further violation of formal time-step restrictions. Numerical experimentation has shown that if the local component Courant numbers do not exceed about 0·2, instabilities do not develop; this is an order of magnitude larger than the value suggested by equation (63) in the test problems considered here.

Variable grids

For clarity, the development of SHARP has been based on the assumption of a uniform grid in each co-ordinate direction. Various levels of generalization are possible. For example, in two dimensions it is a simple matter to extend the formulae to a uniform rectangular grid, $\Delta x = \text{const}$, $\Delta y = \text{const} \neq \Delta x$; and similarly in three dimensions. This is merely reflected in the definition of individual component Courant numbers (and diffusion parameters). The next level of generalization involves locally expanding (or contracting) rectangular grids, with 'expansion ratios' such as $r_x = \Delta x_{i+1}/\Delta x_i$, etc. In principle, one could set up analogous formulae for ϕ_f incorporating r_x, r_y (and r_z in three dimensions), as has been done for QUICK[2,25] using a different notation. However, it turns out that, for QUICK, simply using the constant-grid-spacing formulae on a variable grid results in negligible errors, provided the adjacent mesh width ratios lie within the range $0{\cdot}8 \sim 1{\cdot}25$, i.e. up to approximately a 125% local expansion ratio.[4] This gives a wide range of flexibility in designing variable rectangular meshes without going to the added complexity of variable-grid formulae. Since this conclusion was based on a Taylor series expansion about control-volume faces, and is therefore related to QUICK's NVD behaviour near $\tilde{\phi}_C = 0{\cdot}5$, the

same conclusion must be reached regarding SHARP. The extension to non-rectangular quadrilateral grids is not yet documented; however, it is reasonable to speculate that 'mild' distortion would not result in significant errors, even though the formal order of accuracy is reduced.

TEST PROBLEM RESULTS

The oblique-step test

Figure 8 shows the well known bench-mark test problem consisting of pure convection of an upstream transverse step profile in a scalar field imposed at the inflow boundaries of a (square) computational domain, in this case

$$\Delta x = \Delta y = \tfrac{1}{25}. \tag{64}$$

There are two additional rows of pseudo-nodes upstream of the inflow boundaries, and one additional set downstream. The convecting velocity is of constant magnitude and flows at the same angle θ, oblique to the grid, everywhere. The location of the boundary step is chosen so that the exact convected step passes through the midpoint of the grid, for reference. Note that $\phi = 0{\cdot}5$ along the step itself, whereas $\phi \equiv 1$ everywhere above and $\phi \equiv 0$ below, as indicated.

For $\theta = 45°$ the exact solution is shown in orthographic projection in Figure 9. Note that this particular computer plot routine interpolates linearly between specified grid point values. Figure 10 gives the results for $\theta = 45°$ using classical first-order upwinding for all CV face fluxes. Clearly this is grossly in error owing to the artificial cross-grid diffusion inherent in this method. A quantitative indication of the error is given by

$$\text{ERROR} = \sum |\phi_{\text{computed}} - \phi_{\text{exact}}| \tag{65}$$

summed over all computed (interior) grid points; the magnitude is noted in the figure captions in each case. Figure 11 gives the corresponding results for second-order upwinding. Although the main rise is considerably steeper than first-order, and the ERROR much smaller, the most obvious feature is the (antisymmetrical) pattern of overshoots—of considerable magnitude! This is a serious problem, and one that needs to be addressed by research groups propounding the use of second-order upwinding as a general-purpose convection solver.[4,5] In fact second-order upwinding at this angle gives larger overshoots than QUICK, as seen in Figure 12. The QUICK and second-order upwind results are qualitatively similar; but note that QUICK's step resolution is considerably steeper, and compare the quantitative ERROR magnitudes. Finally, for this 45°

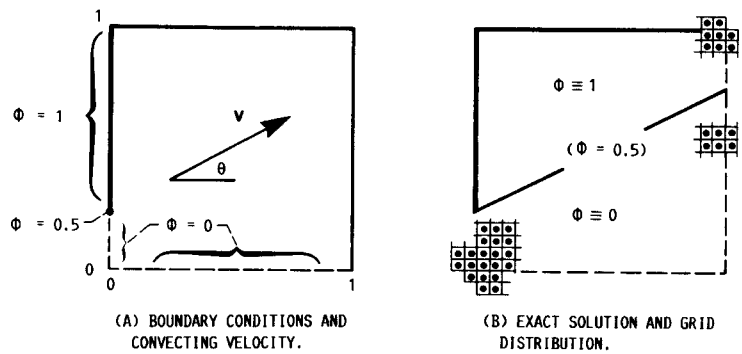

Figure 8. The oblique-step test: (a) boundary conditions and convecting velocity; (b) exact solution and grid distribution

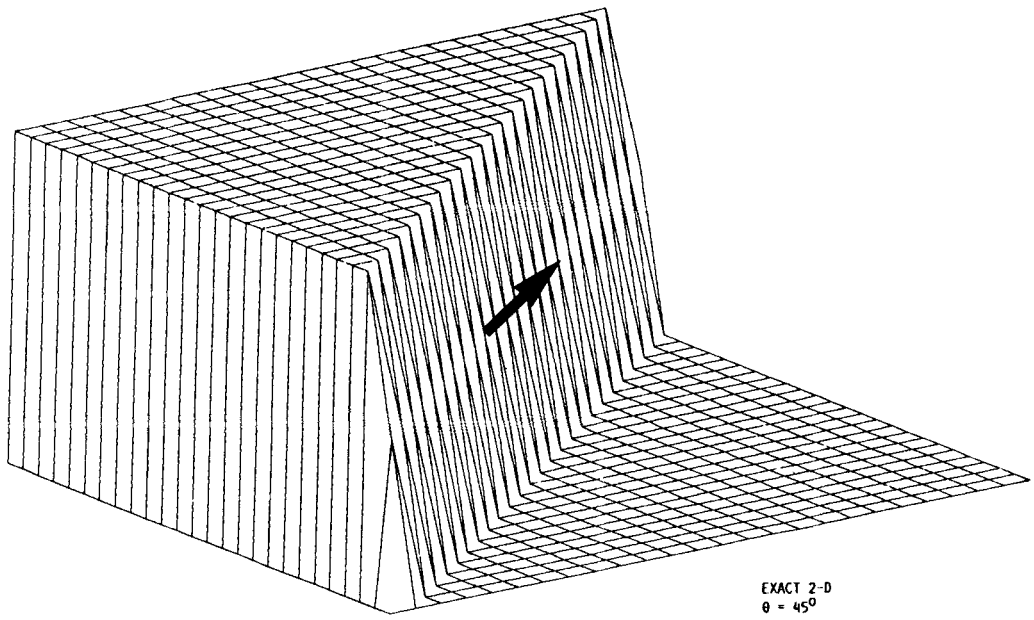

Figure 9. Three-dimensional representation of $\phi(x, y)$ for the exact solution of the oblique-step test for $\theta = 45°$

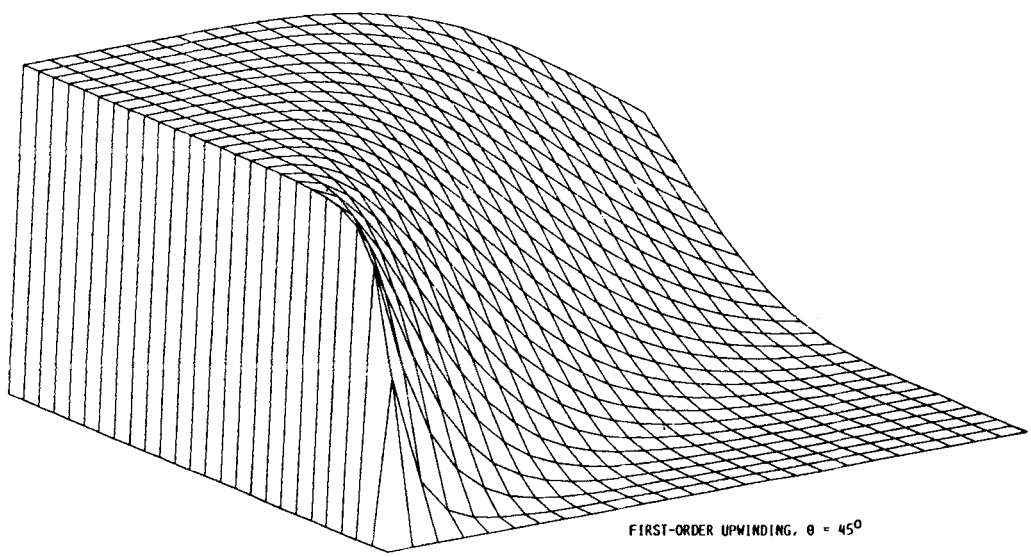

Figure 10. Oblique-step test results for first-order upwinding, $\theta = 45°$; ERROR = 68·2

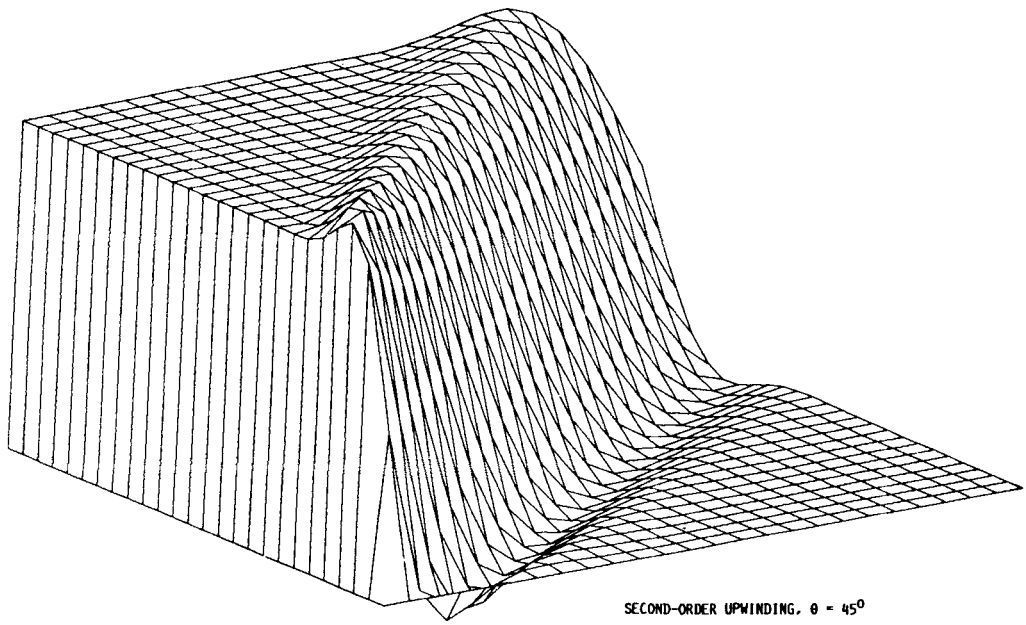

Figure 11. Oblique-step test results for second-order upwinding, $\theta = 45°$; ERROR = 24·4

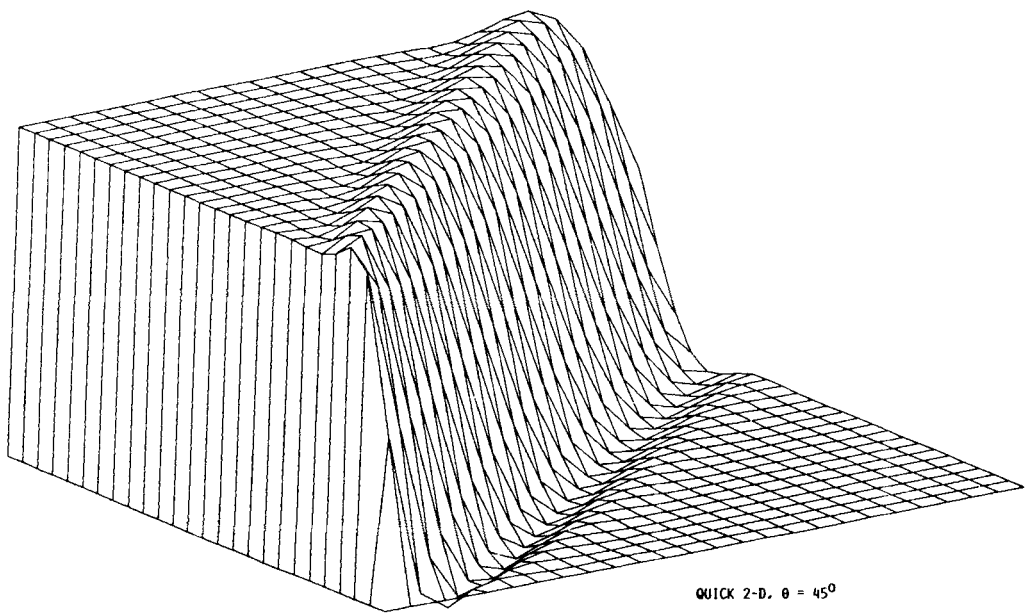

Figure 12. Oblique-step test results for third-order upwinding (QUICK), $\theta = 45°$; ERROR = 16·6

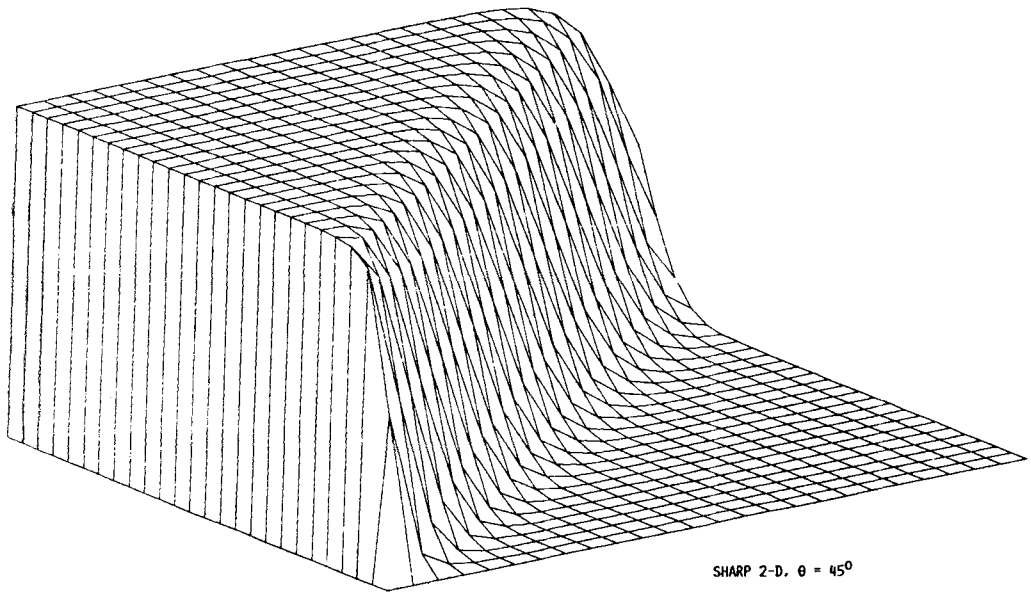

Figure 13. Oblique-step test results for the simple high-accuracy resolution program (SHARP), $\theta = 45°$; ERROR = 16·0

angle, Figure 13 gives the SHARP results—essentially the same steep resolution as QUICK, but with the overshoots 'clipped off' (and smoothed) to give absolutely monotonic simulation. Note the drop in ERROR relative to QUICK.

Of course 45° is a special angle (actually the worst case for first-order upwinding in terms of ERROR magnitude), so two other angles will be considered:

$$\theta = \tan^{-1}(\tfrac{2}{3}) \approx 34° \tag{66}$$

and

$$\theta = \tan^{-1}(\tfrac{3}{2}) \approx 56°. \tag{67}$$

The results—again for the exact solution, first-order upwinding, second-order upwinding, QUICK and SHARP—are shown in Figures 14–18 respectively for $\theta = 34°$ and in Figures 19–23 respectively for $\theta = 56°$. In each case first-order upwinding is artificially diffusive, second-order upwinding and QUICK are oscillatory with much lower ERROR, but SHARP always gives uniformly steep and monotonic results, essentially independent of flow-to-grid angle.

DISCUSSION AND FORECAST

SHARP represents a new generation of multi-dimensional monotonic convective solvers of high formal accuracy (in this case third-order). Other similar schemes can be constructed by devising alternate non-linear characteristics in the normalized variable diagram. For example, Gaskell and Lau's Sharp Monotonic Algorithm for Realistic Transport (SMART) is based on a piecewise linear characteristic[28] consisting of the QUICK line for the bulk of the monotonic range in $\tilde{\phi}_C$, but deviating *via ad hoc* straight-line segments to pass through (0, 0) and (1, 1) in the NVD. SMART and SHARP give virtually identical results for critical steady two-dimensional pure-convection problems such as the oblique-step test. These schemes are similar in some respects to certain types

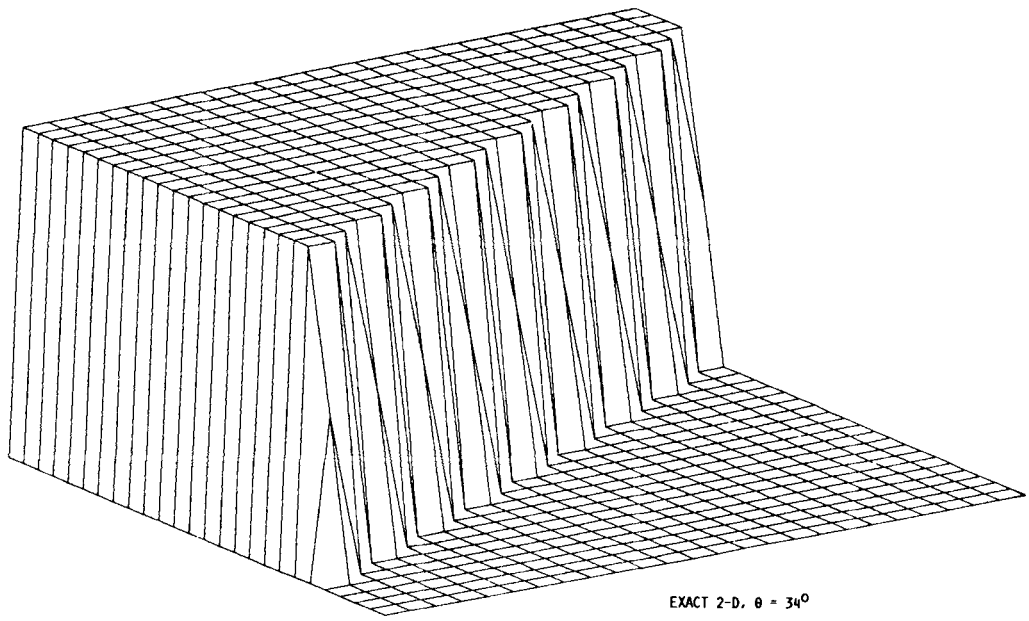

Figure 14. Exact solution for $\theta = 34°$

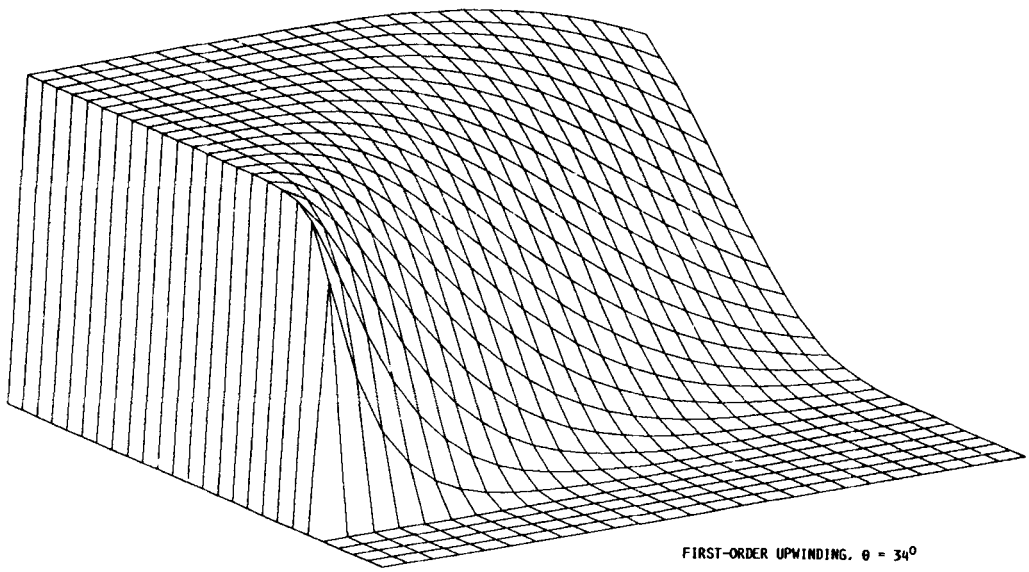

Figure 15. Oblique-step test results for first-order upwinding, $\theta = 34°$; ERROR = 63·8

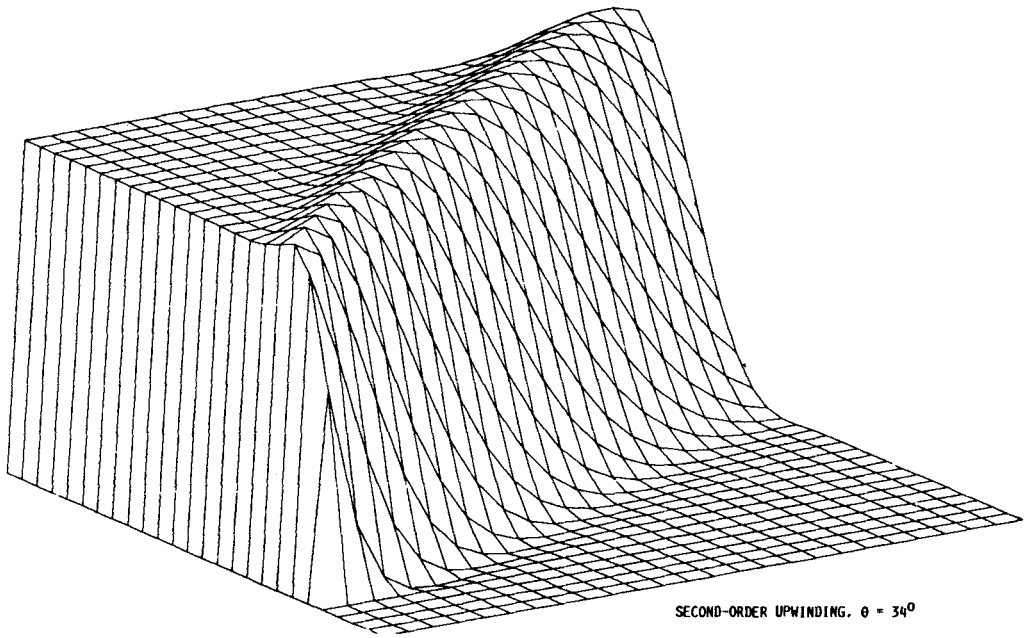

Figure 16. Oblique-step test results for second-order upwinding, $\theta = 34°$; ERROR = 28·7

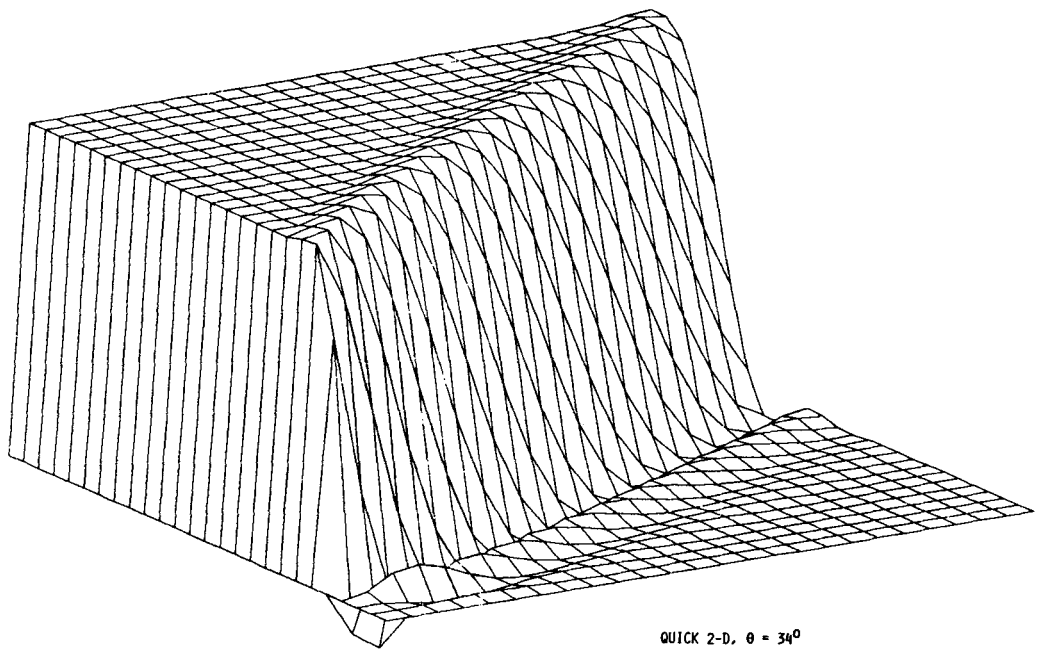

Figure 17. Oblique-step test results for QUICK, $\theta = 34°$; ERROR = 23·4

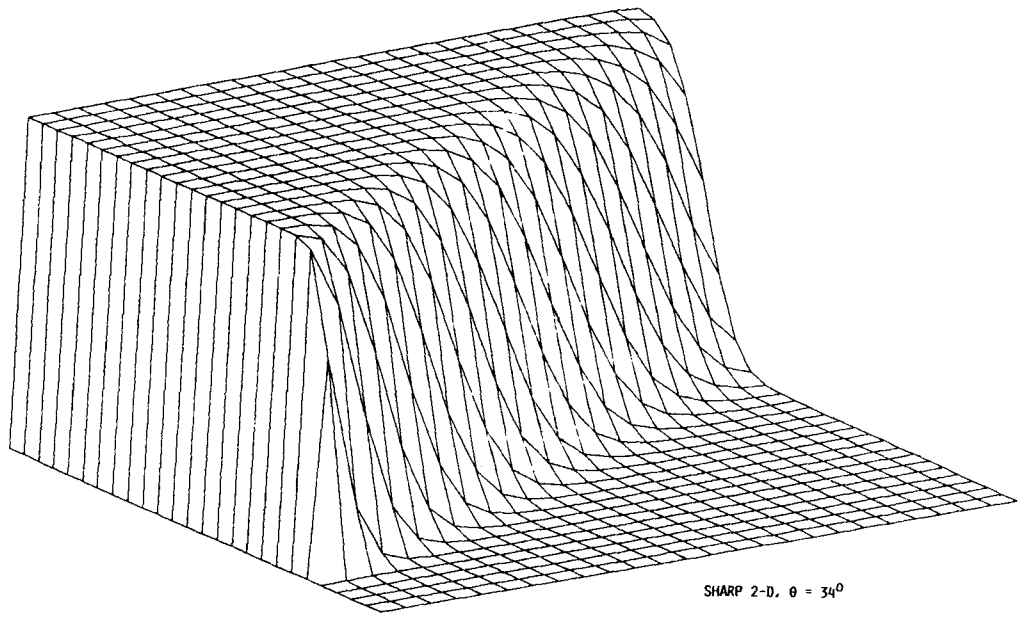

Figure 18. Oblique-step test results for SHARP, $\theta = 34^{\circ}$; ERROR = 19·4

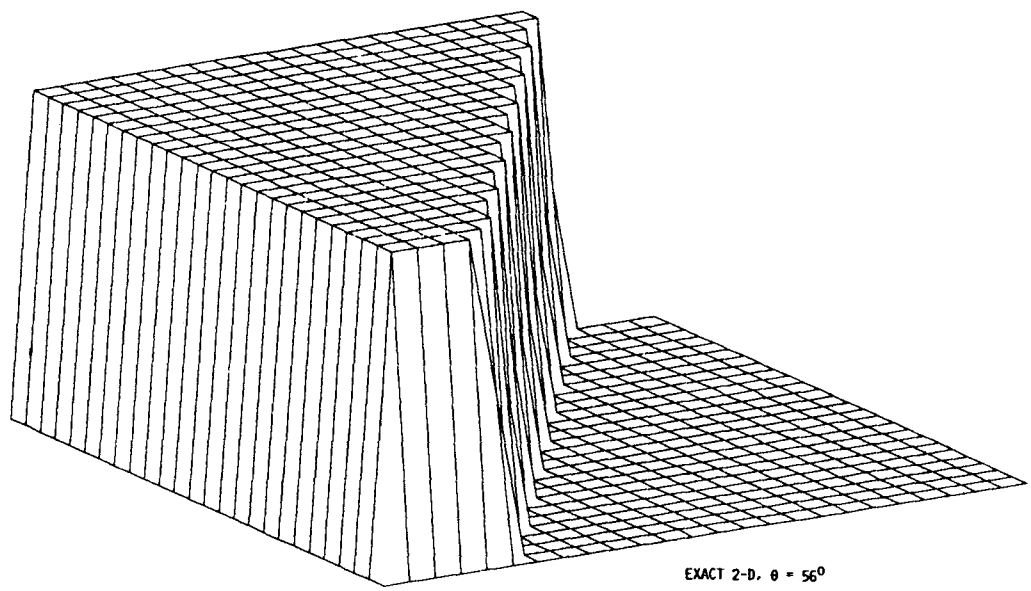

Figure 19. Exact solution for $\theta = 56^{\circ}$

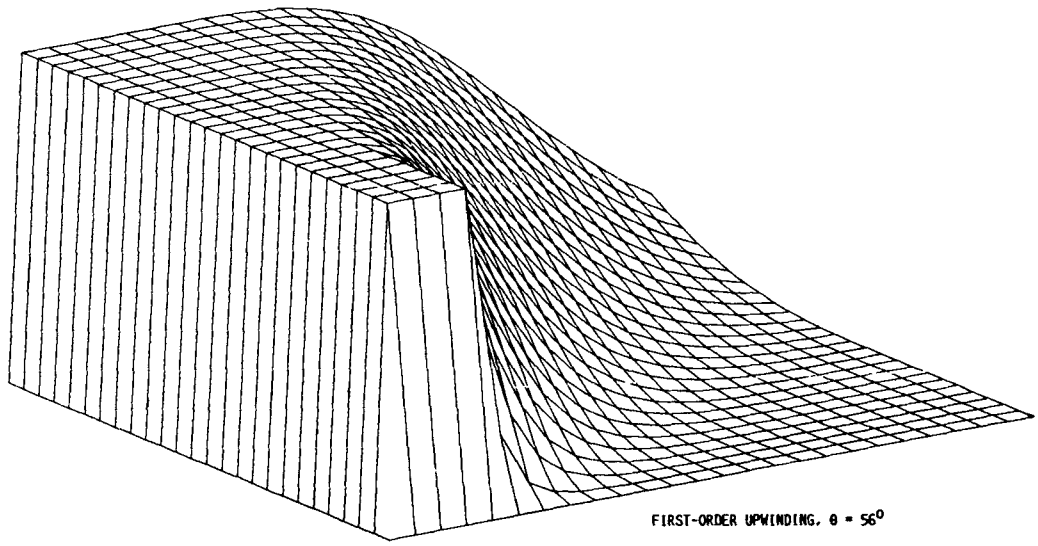

Figure 20. Oblique-step test results for first-order upwinding, $\theta = 56°$; ERROR = 63·8

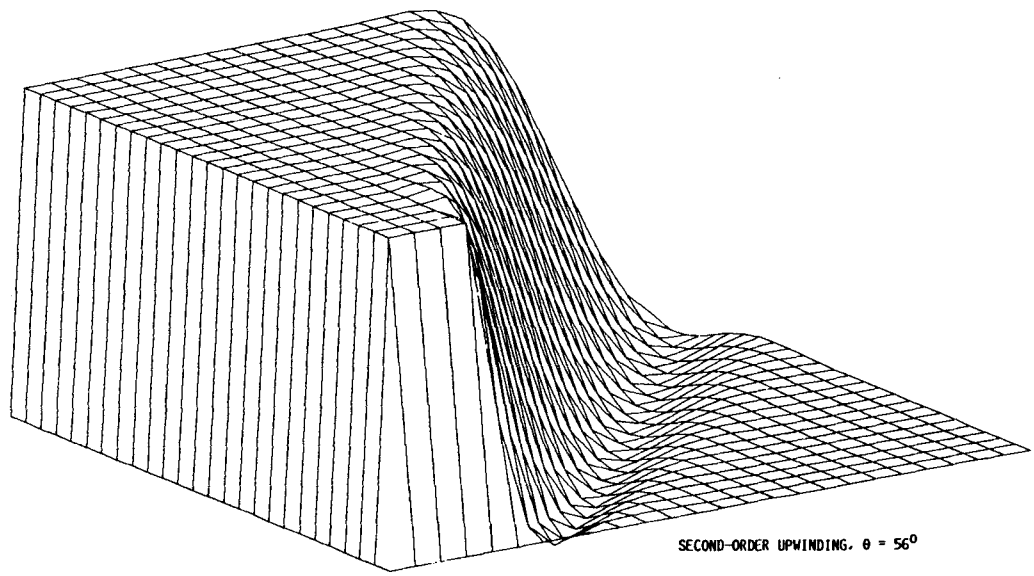

Figure 21. Oblique-step test results for second-order upwinding, $\theta = 56°$; ERROR = 28·7

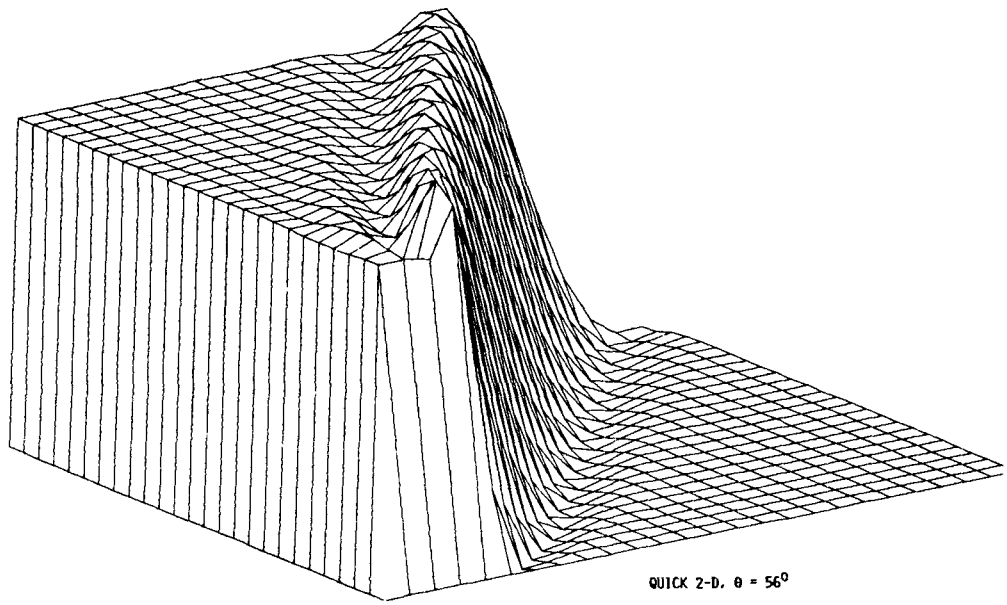

Figure 22. Oblique-step test results for QUICK, $\theta = 56°$; ERROR = 23·4

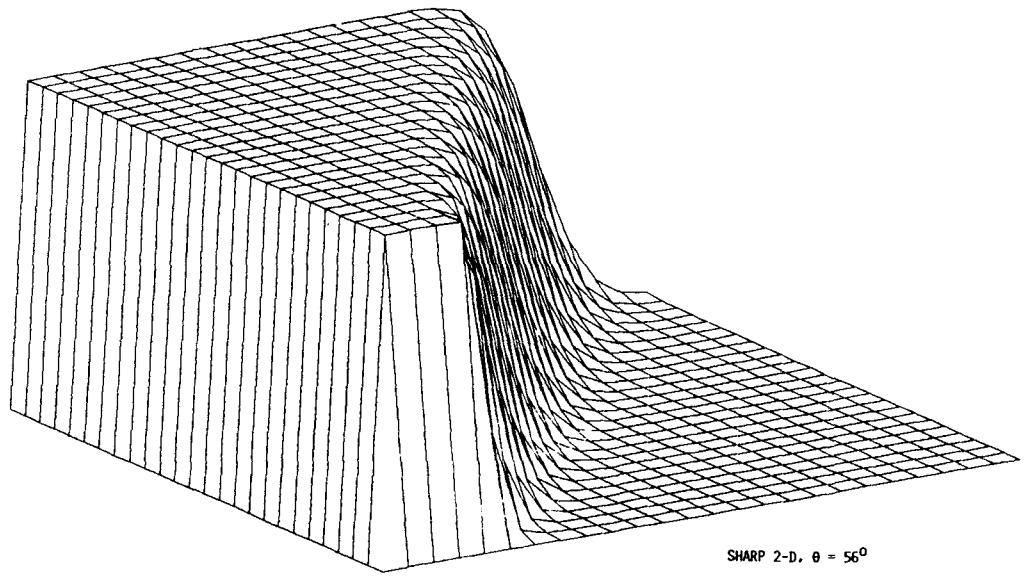

Figure 23. Oblique-step test results for SHARP, $\theta = 56°$; ERROR = 19·4

of flux limiter and so-called 'TVD' schemes developed for simulating shock phenomena in inviscid compressible flows. In fact there is a one-to-one correspondence between the normalized variable diagram and the flux limiter *versus* gradient ratio diagram discussed, for example, by Sweby.[29] It is not difficult to show that the flux limiter factor, FLF (Sweby's φ), is related to the normalized variables used here by

$$\mathrm{FLF}=\frac{\tilde{\phi}_{\mathrm{f}}-\tilde{\phi}_{\mathrm{C}}}{\frac{1}{2}(1-\tilde{\phi}_{\mathrm{C}})} \tag{68}$$

and that the gradient ratio r is given by

$$r=\frac{\tilde{\phi}_{\mathrm{C}}}{1-\tilde{\phi}_{\mathrm{C}}}. \tag{69}$$

Note that the important region near $\tilde{\phi}_{\mathrm{C}}=1$ is banished to large (positive or negative) r-values in Sweby's diagram, whereas the behaviour of the $\tilde{\phi}_{\mathrm{f}}(\tilde{\phi}_{\mathrm{C}})$ characteristic is immediately obvious in the NVD used here. In terms of un-normalized variables, equation (68) is simply

$$\mathrm{FLF}=\frac{\phi_{\mathrm{f}}-\phi_{\mathrm{C}}}{\phi_{\mathrm{f}}^{\mathrm{CEN}}-\phi_{\mathrm{C}}}, \tag{70}$$

where the numerator is the difference between the modelled face value ϕ_{f} and first-order upwinding ϕ_{C}, and the denominator is the difference between second-order central differencing $\phi_{\mathrm{f}}^{\mathrm{CEN}}=\frac{1}{2}(\phi_{\mathrm{D}}+\phi_{\mathrm{C}})$ and first-order upwinding.

In unsteady flows one can obtain the central difference time-averaged (Lax–Wendroff) CV face value from

$$\phi_{\mathrm{f}}^{\mathrm{LW}}=\phi_{\mathrm{f}}^{\mathrm{CEN}}-c(\phi_{\mathrm{f}}^{\mathrm{CEN}}-\phi_{\mathrm{C}}), \tag{71}$$

where c is the Courant number. If one makes the same (second-order time-accurate) assumption for the non-linear face value, averaged over time,

$$\hat{\phi}_{\mathrm{f}}=\phi_{\mathrm{f}}-c(\phi_{\mathrm{f}}-\phi_{\mathrm{C}}), \tag{72}$$

then equation (70) can be written, cancelling the factor $1-c$, as

$$\mathrm{FLF}=\frac{\hat{\phi}_{\mathrm{f}}-\phi_{\mathrm{C}}}{\phi_{\mathrm{f}}^{\mathrm{LW}}-\phi_{\mathrm{C}}}, \tag{73}$$

which, of course, is the basic definition of the flux limiter factor. This means that many of the flux limiter schemes previously developed for unsteady (one-dimensional) gas dynamics will be applicable to steady multi-dimensional highly convective flows as well, using the conservative control-volume formulation described here.

It now appears possible to obtain much better resolution of discontinuities by using non-linear schemes of even higher-order accuracy, in the sense of using more than three grid points (normal to control-volume faces) in estimating local fluxes. Whether this is based on flux-limited higher-order polynomial schemes or more sophisticated forms of (non-polynomial) interpolation, the strategy of using a robust scheme, such as third-order upwinding, in the bulk of the flow domain and switching to the (presumably) more costly computation only where necessary (in thin layers) will remain highly cost-effective.

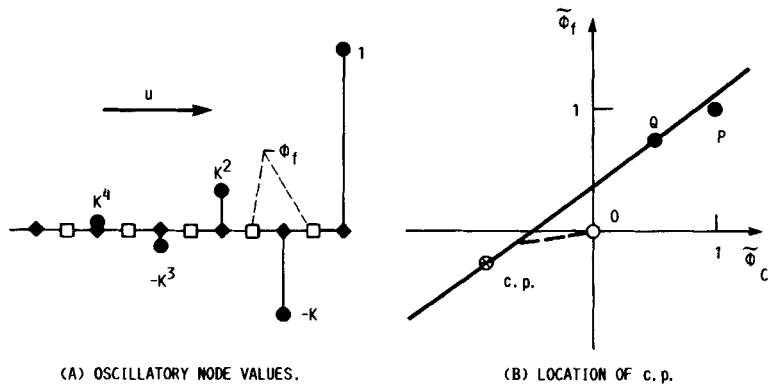

Figure 24. Oscillatory critical point for QUICK: (a) node values; (b) NVD location

APPENDIX

Consider a linear characteristic in the NVD of the form

$$\tilde{\phi}_f = S\tilde{\phi}_C + I. \tag{74}$$

In one-dimensional simulations, if oscillations occur, they will take the form of an alternating geometric series, decaying upstream: $\phi_i = 1$, $\phi_{i-1} = -K$, $\phi_{i-2} = K^2$, etc. Let $\phi_D = 1$; then $\phi_C = -K$, $\phi_U = K^2$. The corresponding normalized variable is

$$\tilde{\phi}_C^* = \frac{\phi_C - \phi_U}{\phi_D - \phi_U} = \frac{-K - K^2}{1 - K^2} = -\frac{K}{1-K}, \tag{75}$$

where the 'star' signifies a critical value of $\tilde{\phi}_C$ (corresponding to the oscillatory behaviour). The accompanying face value is $\phi_f^* = 0$, as seen in Figure 24(a); thus the normalized face value becomes

$$\tilde{\phi}_f^* = S\left(\frac{-K}{1-K}\right) + I = \frac{\phi_f^* - \phi_U}{\phi_D - \phi_U} = \frac{-K^2}{1-K^2}. \tag{76}$$

This gives a quadratic equation for K, the appropriate root being

$$K = \frac{S - \sqrt{S^2 - 4I(1-S-I)}}{2(1-S-I)}. \tag{77}$$

For example, for QUICK ($S = 0{\cdot}75$, $I = 0{\cdot}375$)

$$K(\text{QUICK}) = 2\sqrt{3} - 3 = 0{\cdot}4641 \tag{78}$$

and the critical point is given by

$$\tilde{\phi}_C^*(\text{QUICK}) = \sqrt{(3/2)} = -0{\cdot}8660 \tag{79}$$

and

$$\tilde{\phi}_f^*(\text{QUICK}) = -\tfrac{3}{8}(\sqrt{3} - 1) = -0{\cdot}2745 \tag{80}$$

as shown in Figure 24(b).

Note that for second-order central differencing ($S=0{\cdot}5$, $I=0{\cdot}5$), $K=1$, implying undamped oscillation. Also, if the characteristic passes through $O(I=0)$, then $K\equiv 0$; i.e. perfect step resolution. Finally, if $I<0$ (i.e. the characteristic passes through the fourth quadrant), K is negative, implying a non-oscillatory geometric decay or artificial diffusion. It should be clear that any linear characteristic passing through the second quadrant ($I>0$) will have a corresponding critical point in the third quadrant. More general results concerning non-linear characteristics can be determined. In particular, any (in general, non-linear) characteristic passing through the second quadrant will have a potentially oscillatory critical point in the third quadrant. This can be seen by imagining a local first-order Taylor expansion of the form of equation (74) about candidate critical points; provided the trajectory enters the third quadrant from the second, there will always be values of S and I satisfying equations (75), (76) and (77) at some point on the trajectory in the third quadrant. Trajectories entering the third quadrant through O or the fourth quadrant may also have critical points, as would the scheme shown dashed in Figure 24(b), which rejoins the QUICK scheme above its critical point. Clearly the most satisfactory design is to pass through O, staying low enough to avoid potential critical points. This is the case with the *ad hoc* linear extension chosen in constructing the EULER–QUICK scheme.

REFERENCES

1. R. F. Warming and R. M. Beam, 'Upwind second-order difference schemes and applications in aerodynamic flows', *AIAA J.*, **14**, 1241–1249 (1976).
2. B. P. Leonard, 'A stable and accurate convective modelling procedure based on quadratic upstream interpolation', *Comput. Methods Appl. Mech. Eng.*, **19**, 59–98 (1979).
3. A. D. Gosman and W. M. Pun, 'Calculation of recirculating flows', *Report No. HTS/74/2*, Department of Mechanical Engineering, Imperial College, London, 1974.
4. I. P. Castro and J. M. Jones, 'Studies in numerical computations of recirculating flows', *Int. j. numer. methods fluids*, **7**, 793–823 (1987).
5. A. D. Burns, I. P. Jones, J. R. Kightley and N. S. Wilkes, 'The implementation of a finite difference method for predicting incompressible flows in complex geometries', in C. Taylor *et al.* (eds), *Numerical Methods in Laminar and Turbulent Flow, Vol. 5*, Pineridge Press, Swansea, 1987, pp. 339–350.
6. P. G. Huang, B. E. Launder and M. A. Leschziner, 'Discretization of nonlinear convection processes: a broad range comparison of four schemes', *Comput. Methods Appl. Mech. Eng.*, **48**, 1–24 (1985).
7. T. Han, J. A. C. Humphrey and B. E. Launder, 'A comparison of hybrid and quadratic upstream differencing in high Reynolds number elliptic flows', *Comput. Methods Appl. Mech. Eng.*, **29**, 81–95 (1981).
8. J. A. C. Humphrey, H. Iacovides and B. E. Launder, 'Some numerical experiments on developing laminar flow in circular-sectioned bends', *J. Fluid Mech.*, **154**, 357–375 (1985).
9. R. A. Beier, J. de Ris and H. R. Baum, 'Accuracy of finite-difference methods in recirculating flows', *Numer. Heat Transfer*, **6**, 283–302 (1983).
10. J. Azzola, J. A. C. Humphrey, H. Iacovies and B. E. Launder, 'Developing turbulent flow in a U-bend of circular cross-section: measurement and computation', *J. Fluids Eng.*, **108**, 214–221 (1986).
11. R. E. Phillips and F. W. Schmidt, 'Multigrid techniques for the solution of the passive scalar advection–diffusion equation', *Numer. Heat Transfer*, **8**, 25–43 (1985).
12. D. L. Rhode, J. A. Demko, U. K. Traegner, G. L. Morrison and S. R. Sobolik, 'Prediction of incompressible flow in labyrinth seals', *J. Fluids Eng.*, **108**, 19–25 (1986).
13. S. K. Aggarwal, 'Numerical study of convection–diffusion–reaction equations for large Damkohler and cell Reynolds numbers', *Numer. Heat Transfer*, **11**, 143–164 (1987).
14. C. Y. Perng and R. L. Street, 'Improved numerical codes for solving three-dimensional unsteady flows',in C. Taylor *et al.* (eds), *Numerical Methods in Laminar and Turbulent Flow, Vol. 5*, Pineridge Press, Swansea, 1987, 12–22.
15. A. W. Neuberg, 'Error estimates and convergence acceleration of different discretization schemes', in C. Taylor *et al.* (eds), *Numerical Methods in Laminar and Turbulent Flow, Vol. 5*, Pineridge Press, Swansea, 1987, pp. 91–101.
16. P. H. Gaskell, A. K. C. Lau and N. G. Wright, 'Two efficient solution strategies for use with high order discretisation schemes, in the simulation of fluid flow problems', in C. Taylor *et al.* (eds), *Numerical Methods in Laminar and Turbulent Flow, Vol. 5*, Pineridge Press, Swansea, 1987, pp. 210–220.
17. D. F. G. Durão and J. C. F. Pereira, 'A numerical–experimental study of confined unsteady laminar flow around a squared obstacle', in C. Taylor *et al.* (eds), *Numerical Methods in Laminar and Turbulent Flow, Vol. 5*, Pineridge Press, Swansea, 1987, pp. 261–272.

18. J. A. Demko, G. L. Morrison and D. L. Rhode, 'Effect of shaft rotation on the incompressible flow in a labyrinth seal', in C. Taylor *et al.* (eds), *Numerical Methods in Laminar and Turbulent Flow, Vol. 5*, Pineridge Press, Swansea, 1987, pp. 508–520.
19. L. J. Johnston, 'A numerical method for three-dimensional compressible turbulent boundary-layer flows', in C. Taylor *et al.* (eds), *Numerical Methods in Laminar and Turbulent Flow, Vol. 5*, Pineridge Press, Swansea, 1987, pp. 1421–1435.
20. M. A. Leschziner and E. G. Hoholis, 'On the influence of the numerical approximation of convection in the computation of 3D jet injection into an IC-engine combustion-chamber model', in C. Taylor *et al.* (eds), *Numerical Methods in Laminar and Turbulent Flow, Vol. 5*, Pineridge Press, Swansea, 1987, pp. 1436–1447.
21. S. A. Syed, A. D. Gosman and M. Peric, 'Assessment of discretization schemes to reduce numerical diffusion in th calculation of complex flows', *Paper No. AIAA-85-0441, AIAA 23rd Aerospace Sciences Meeting*, Reno, Nevada, January 1985.
22. P. G. Huang, Department of Mechanical Engineering and Engineering Mechanics, Michigan Technological University, personal communication.
23. M. A. Leschziner and W. Rodi, 'Calculation of annular and twin parallel jets using various discretization schemes and turbulence-model variations', *J. Fluids Eng.* **103,** 352–360 (1981).
24. J. B. Goodman and R. J. LeVeque, 'On the accuracy of stable schemes for 2D scalar conservation laws', *Math. Comput.* **45,** 15–21 (1985).
25. B. P. Leonard, 'Elliptic systems: finite-difference method IV', in W. J. Minkowycz *et al.* (eds), *Handbook of Numerical Heat Transfer*, Wiley, New York, 1988, Ch. 9, pp. 347–378.
26. B. P. Leonard, 'Note on the von Neumann stability of the explicit FTCS convective diffusion equation', *Appl. Math. Modelling*, **4,** 401–403 (1980).
27. S. Paollucci and D. R. Chenoweth, 'A note on the stability of the explicit finite differenced transport equation', *J. Comput. Phys.* **47,** 489–496 (1982).
28. P. H. Gaskell and A. K. C. Lau, 'Curvature compensated convective transport: SMART, a new boundedness preserving transport algorithm', *Int. J. Numer. Methods Fluids*, **8,** 617–641 (1988).
29. P. K. Sweby, 'High resolution schemes using flux limiters for hyperbolic conservation laws', *SIAM J. Numer. Anal.*, **21,** 995–1011 (1984).